

A Thermoacoustic Imaging System for Non-Invasive and Non-Destructive Root Phenotyping

Ajay Singhvi, *Graduate Student Member, IEEE*, Aidan Fitzpatrick, *Graduate Student Member, IEEE*, Johannes Daniel Scharwies, José R. Dinneny, and Amin Arbabian, *Senior Member, IEEE*

Abstract—Information about the root system architecture of plants is of great value in modern crop science. However, there is a dearth of tools that can provide field-scale measurements of below-ground parameters in a non-destructive and non-invasive fashion. In this paper, we propose a multi-modal, non-contact thermoacoustic sensing system to address this measurement gap and discuss various system design aspects in the context of below-ground sensing. We also demonstrate the first thermoacoustic images of plant material (potatoes) in a soil medium, with the use of highly sensitive capacitive micromachined ultrasound transducers enabling non-contact detection and *cm*-scale image resolution. Finally, we show high correlation (adj. $R^2 = 0.95$) between the measured biomass content and the reconstructed thermoacoustic images of the potato tubers.

Index Terms—Below-ground sensing, capacitive micromachined ultrasonic transducer, CMUT, non-contact, phenotyping, ultrasound, thermoacoustics

I. INTRODUCTION

POPULATION growth, resource depletion, and climate change pose an increasing threat to global food security, with a significant increase in crop production and efficiency needed to meet growing food demands [1]. Plant phenotyping [2], which refers to the quantification of a crop’s anatomical, physiological, biochemical and ontogenetical properties, is one of most important tools that can be leveraged to tackle these challenges. Phenotyping technologies have tremendous utility for crop breeding, providing a data-driven means to identify plant cultivars with desirable characteristics such as higher yield, drought and disease resistance, and improved nutrient profiles [3]. Precision agriculture also utilizes such tools for intelligent crop management, better irrigation scheduling, and targeted fertilizer use to improve resource efficiency [4].

Satellite and drone based remote-sensing systems deploying spectral, optical and thermal sensors are already widely used for high-throughput, field-based phenotyping of above-ground traits [5]. However, there is a dearth of tools that can provide high-throughput, non-destructive, and field-based phenotyping of below-ground traits [6]. Filling this measurement gap would enable plant breeders and biologists to develop new root-focused cultivars with improved root system architectures which could be the impetus for a second Green Revolution that helps overcome the critical challenges we face today [7].

This work was supported by Advanced Research Projects Agency-Energy Grant DE-AR0000825, sponsored by the ROOTS program.

A. Singhvi, A. Fitzpatrick, and A. Arbabian are with the Department of Electrical Engineering, Stanford University, Stanford, CA 94305 USA (e-mail: asinghvi@stanford.edu).

J.D. Scharwies and J. R. Dinneny are with the Department of Biology, Stanford University, Stanford, CA 94305 USA.

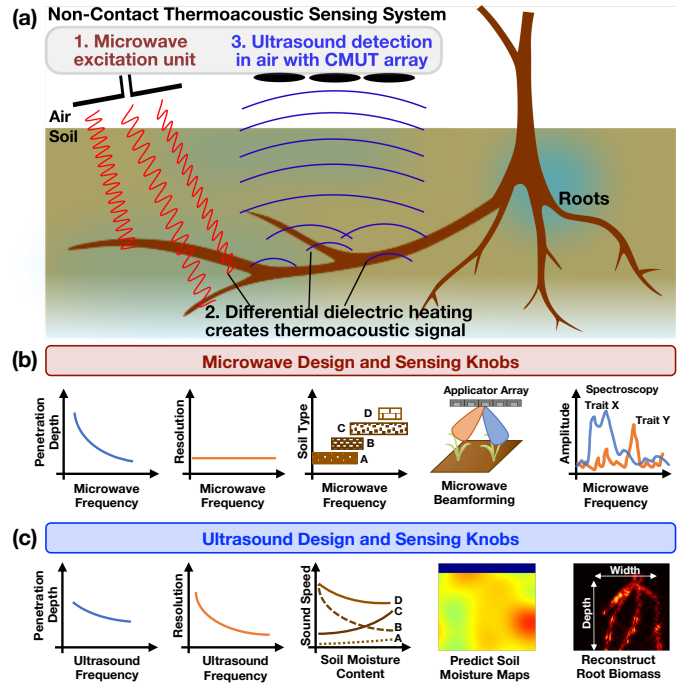


Fig. 1. Conceptual view of proposed non-contact thermoacoustic below-ground sensing system along with the multi-modal design and sensing knobs

The opaque nature of soil along with the complex, heterogeneous below-ground environment makes the development of in-situ below-ground sensing technologies far more challenging than their above-ground counterparts. Most root phenotyping technologies that are deployed today are either high-resolution, non-destructive approaches that only work well in controlled settings or low-throughput field-based approaches that are invasive, labor-intensive, and often destructive [6]. Thus, there are ongoing efforts to develop a high-throughput field-based root phenotyping system that can provide non-destructive, dynamic measurements of below-ground traits [8].

Towards that end, we propose a non-contact thermoacoustic (NCTA) sensing system that addresses many of the above challenges. It relies on the thermoacoustic (TA) effect, wherein microwave illumination results in differential heating and in-turn generates acoustic or ultrasonic (US) pressure waves at interfaces with dielectric contrast [9]. In this application, as conceptually illustrated in Fig. 1a, TA waves are generated at root-soil interfaces, with non-contact detection using highly sensitive air-coupled Capacitive Micromachined Ultrasound Transducers (CMUTs) [10], paving the way for high-throughput, autonomous sensing at large spatial scales.

The multi-modal nature of the system enables decoupling of the excitation and detection mechanisms and provides many degrees-of-freedom for system design as well as opportunities to sense a variety of below-ground traits.

Section II of the paper presents an overview of these design knobs that are instrumental in making the NCTA system a versatile tool that can be effectively deployed for sensing the challenging, heterogeneous below-ground field environment. While prior work [11] has shown the generation of one-dimensional TA signals from synthesized root phantoms in soil, this paper demonstrates the first experimentally captured and reconstructed TA images of plant material embedded in a soil medium in Section III. Specifically, as a proof of concept demonstration of this novel TA imaging system, we focus on the imaging of relatively large (*cm*-scale) potato tubers as a preliminary milestone, while still achieving better resolution than current state-of-the-art non-invasive below-ground imaging systems [12]. Finally, in Section IV we also demonstrate mapping of thermoacoustic data to a parameter of interest, specifically extracting information from the reconstructed TA images and mapping it to ground-truth biomass content as an example application of our proposed sensing system.

II. SYSTEM DESIGN

A. Microwave Excitation Unit

Thermoacoustic Physics. The generation and propagation of acoustic signals via the TA effect is governed by the wave equation [13]:

$$\left(\nabla^2 - \frac{1}{v_s^2} \frac{\partial^2}{\partial t^2}\right) p(r, t) = -\frac{\beta}{C_p} \frac{\partial h(r, t)}{\partial t}, \quad (1)$$

where v_s is the speed-of-sound, $p(r, t)$ is the acoustic pressure at position r and time t , β and C_p are the thermal expansion coefficient and specific heat capacity of the absorbing medium, and $h(r, t)$ is the heating function defined as the EM power absorbed per unit volume. The microwave excitation source, and hence the absorbed EM energy, is modulated at a desired US frequency, in order to generate a TA pressure signal that can be captured using a matched US transducer [9].

Microwave Design Knobs. As seen from (1), the generated TA signals depend on the heating function which is governed by the microwave excitation unit. The choice of microwave frequency plays a major role in the generation of the TA signal via the dielectric contrast, specifically via differences in the dielectric loss factor or complex permittivity between the root and soil at the chosen frequency [11], [14], [15]. Moreover, it also directly controls the penetration depth of the system, since EM attenuation in soil is greater at higher frequencies. Ground Penetrating Radar (GPR) systems are the closest counterpart to the proposed NCTA system but suffer from a fundamental tradeoff between image resolution and penetration depth through the operating frequency, and can only operate reliably in certain soil types [16]. However, the decoupling of the excitation and detection mechanisms in the proposed NCTA system ensures that the image resolution is completely independent of the microwave frequency, enabling the optimal microwave frequency to be chosen purely based

on soil type, the required dielectric contrast between root and soil, and penetration depth as shown schematically in Fig. 1b.

Microwave Sensing Knobs. Microwave applicator arrays, especially with recent advances in silicon and GaN devices enabling the use of portable high-power microwave sources [17], can be used to efficiently beamform energy to desired depths in soil and spatially steer beams for targeted excitation. Moreover, spectroscopic approaches that measure the TA signals at different microwave frequencies can be used as a sensing knob to identify parameters of interest like soil clay composition [18] and soil water content [19].

Microwave Transmitter. In this work, based on available high-power microwave sources as well as prior work demonstrating sufficient contrast at GHz frequencies for a broad range of applications [9], [11], we choose to operate at a microwave frequency of 2.4 GHz with a 1 kW peak power (average power < 5 W) for a proof-of-concept demonstration. An open-ended waveguide, placed in contact with the soil, is used to provide the microwave excitation to the sample used in the imaging experiments. Future iterations of the system could also use non-contact applicator arrays [12].

B. Ultrasound Detection Unit

Non-Contact Detection. To enable field-scale sensing and overcome the challenge of achieving good mechanical coupling at the irregular soil surface, we operate instead at a standoff in air by using highly sensitive air-coupled CMUTs [10]. The CMUTs are instrumental in overcoming the propagation losses in soil as well as the large interface loss as the TA signal travels from the soil to air in the absence of any coupling media [9]. Further, since the CMUTs are silicon compatible devices, they can easily be fabricated at scale as well as interfaced with supporting electronics [20], [21].

Ultrasound Design Knobs. The sensitivity, bandwidth (BW) and operating frequency of the chosen CMUT directly govern the image resolution and SNR (or penetration depth) as shown schematically in Fig. 1c. Like other MEMS based devices, the CMUTs have an inherent sensitivity-BW tradeoff, which we explore experimentally via the use of different CMUT designs in our imaging experiments.

Ultrasound Sensing Knobs. The hybrid nature of the systems adds additional ultrasonic sensing knobs to the NCTA system as shown in Fig. 1c. One such knob leverages the dependence of the speed of sound on soil moisture content [22] to create soil moisture profiles [23]. An ultrasonic detection mechanism also results in the proposed NCTA system outperforming GPR systems in terms of resolution as sound travels much slower than EM waves, with smaller acoustic wavelengths allowing us to resolve finer targets. Image reconstruction algorithms applied on the collected TA data can thus be used to reconstruct relatively high-fidelity below-ground images and map to properties of interest as experimentally detailed in the following sections.

Ultrasound Receivers. We choose three different CMUT designs [10], [24], [25] in this work. The cross sections and impedance models of the CMUTs are shown in Fig. 2a-c. Fig. 2a shows a CMUT with a vacuum gap between the

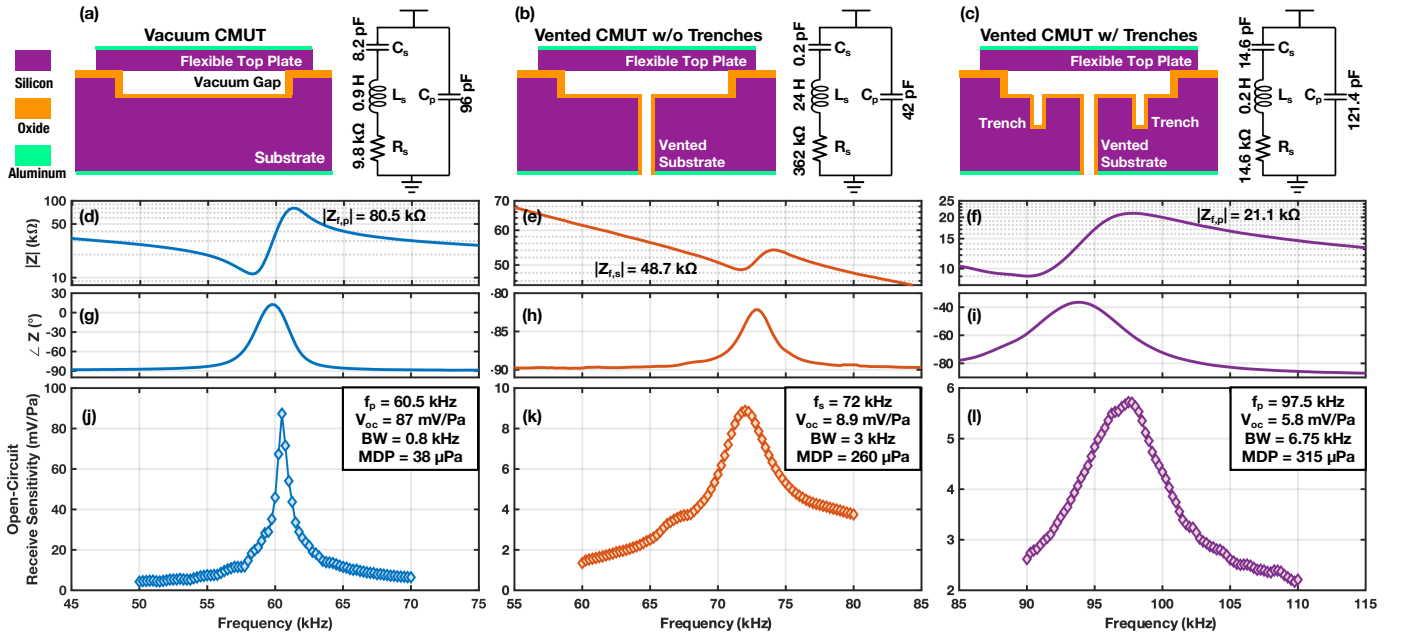


Fig. 2. Three different CMUT designs fabricated and used in this work: vacuum CMUT, vented CMUT without trenches, and vented CMUT with trenches and their (a), (b), (c) Cross-sectional view and impedance model; (d), (e), (f) Measured impedance magnitude; (g), (h), (i) Measured impedance angle; (j), (k), (l) Measured open-circuit sensitivity, bandwidth and minimum detectable pressure.

plate and substrate, designed to maximize sensitivity. Fig. 2b-c show CMUTs wherein damping mechanisms are introduced by etching vias and trenches in the substrate, to widen the CMUT BW for improved imaging resolution, albeit at the cost of some reduction in sensitivity.

Fig. 2d-i show the measured impedance profiles of the CMUT designs. The impedance models inform the design of noise-optimal interfacing electronics for each CMUT using well-known circuit design principles [26]. While most immersion CMUT devices use current-sensing front-ends [27], the low acoustic impedance of air (which often translates to low CMUT resistance) makes it more power and noise efficient to use a voltage amplifying analog front-end (AFE) for some air-coupled CMUTs [20]. We thus use a programmable two-stage voltage amplifying (100-1000 V/V) AFE and on-board filtering to interface with the vacuum CMUT and the vented CMUT with trenches. On the other hand, the relatively high impedance of the vented CMUT without trenches (Fig. 2b, e, h) makes it more noise-optimal to use a current sensing AFE and we thus interface it with a programmable resistive feedback trans-impedance amplifier (gain of $15M-1G\Omega$).

We also conduct pitch-catch experiments in air with a calibrated microphone (GRAS 40 DP) to characterize each CMUT's open-circuit sensitivity (V_{oc}), bandwidth (BW) as well as minimum detectable pressure (MDP) as seen in Fig. 2j-l. The vacuum CMUT has $\approx 10\times$ higher sensitivity than the vented CMUTs, while the vented CMUT with trenches has nearly $10\times$ wider BW than the vacuum CMUT. Note that the vacuum CMUT and vented CMUT with trenches operate at the parallel resonance frequency (f_p) where the electromechanical voltage is maximized, while the vented CMUT without trenches operates at its series resonance frequency (f_s) where the electromechanical current is maximized.

III. TUBER CROP IMAGING

Tuber crops have most of their economic potential stored underground and hence are a favorable candidate to demonstrate the imaging capabilities of our NCTA system. Specifically, we choose to image potato (*Solanum tuberosum* L.) crops since they are the world's most important non-grain food crop [28]. Moreover, potato production currently requires large quantities of water and fertilizer [29], with potato crops being susceptible to disease [30] and facing diminishing yields due to climate change [31] — inefficiencies which could be mitigated by using root phenotyping tools as described in Section I.

A conceptual view of the imaging setup is shown in Fig. 3a. Potato cultivars were harvested and then placed in a 40 cm deep container of Potting Mix (PRO-MIX HP, Premier Tech Horticulture), at depths varying from 10 – 20 cm, with microwave excitation applied through an open-ended waveguide. The CMUT, placed at a 20 cm standoff in air is scanned across a 30 cm swath of soil using a motorized linear stage to synthesize a wide aperture and improve image resolution [9]. The captured A-scan data from across the aperture is then fed into a piece-wise SAR based imaging reconstruction algorithm [9], [32] to reconstruct TA images of the potato tubers.

Fig. 3b-d show ground truth-images of the tubers before they were inserted into the soil, with Fig. 3e-g showing the corresponding reconstructed TA images that match well with the ground-truth, achieving cm -scale image resolution, and outperforming state-of-the-art GPR systems [12]. They also demonstrate the tradeoffs involved in using the three different CMUT designs: the vacuum CMUT could image potatoes at the largest depths, the vented CMUT with trenches offered the best resolution, and the vented CMUT without trenches provided a balance between achievable depth and resolution.

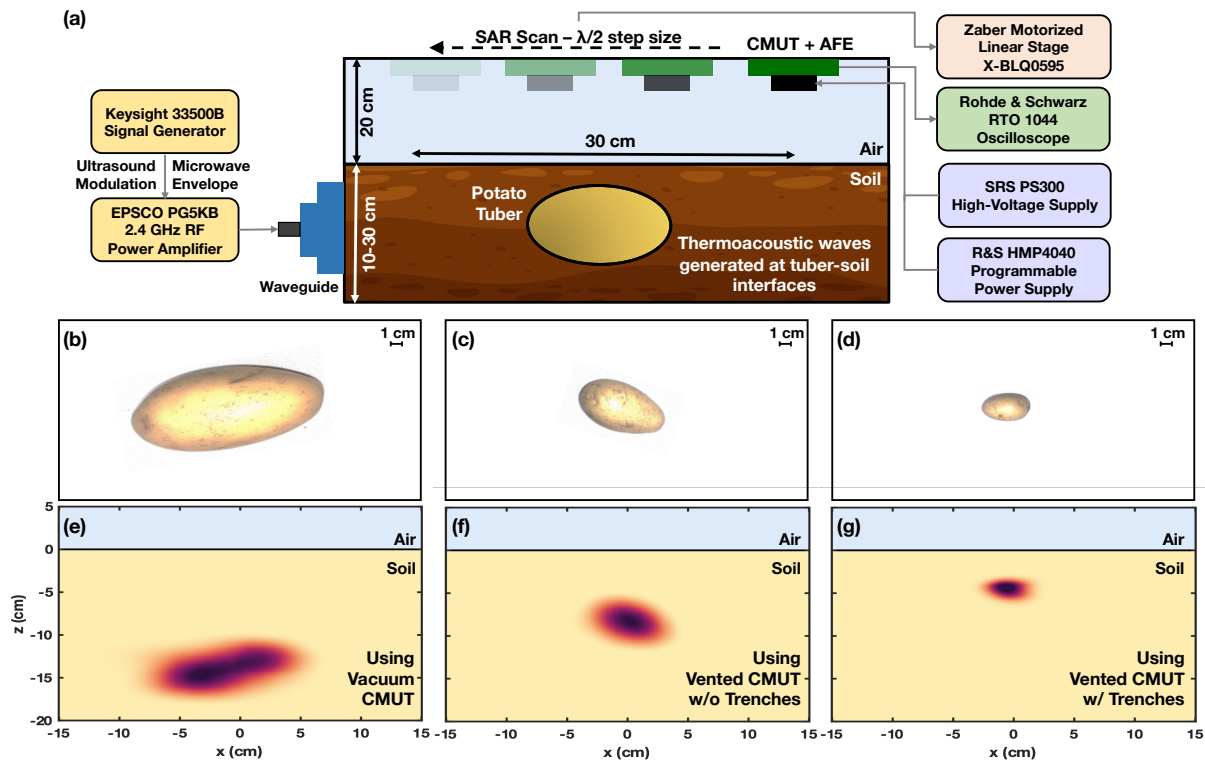


Fig. 3. (a) Experimental setup for non-contact thermoacoustic imaging of potato tubers embedded in soil; (b), (c), (d) Ground-Truth images of potato tubers; (e), (f), (g) Corresponding reconstructed thermoacoustic images.

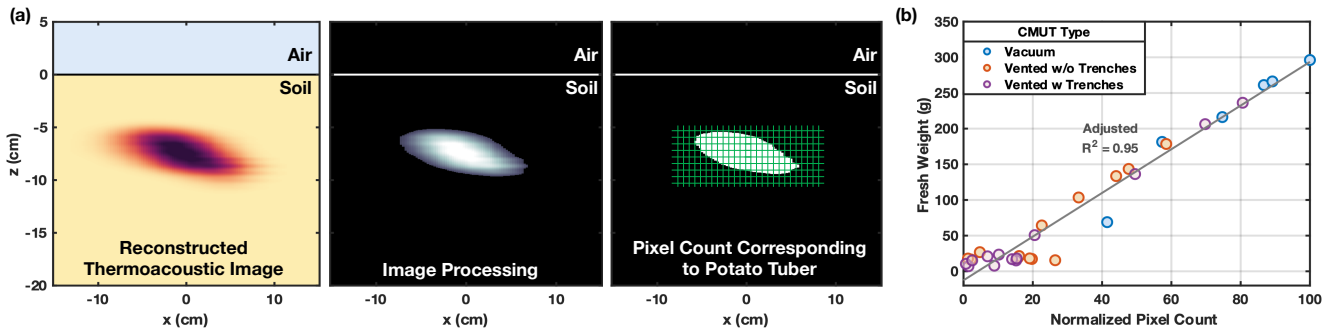


Fig. 4. (a) Image processing pipeline for extracting the number of pixels corresponding to the presence of potato tubers from reconstructed thermoacoustic images; (b) Correlation between extracted pixel count and fresh weight of the imaged potatoes, which serves as a proxy for biomass content.

IV. BIOMASS MAPPING

In addition to end-to-end imaging, phenotyping systems can also be used to extract information about other traits of interest like root system architecture (depth, width, number of roots), soil (moisture, texture, composition), nutrient, and environmental parameters. Such quantitative information is sought after by plant breeders and geneticists to study the impact of genotype, environment, and management ($G \times E \times M$) interactions on the plant cultivars being investigated [33]. Providing actionable, quantitative insights is also important to enable adoption of such technologies in spheres like small-scale farming, that have traditionally lagged behind in adopting such digital solutions [34].

As an example of obtaining such quantitative data, we use the reconstructed TA images to extract information about the potato biomass content. Continuous monitoring of root

biomass could be useful for a number of applications, including but not limited to: identifying the optimal time for harvest, studying and rectifying spatial variations in plant growth in different areas of the field, choosing cultivars with desired traits, and improving resource efficiency via targeted use of fertilizers and intelligent irrigation scheduling depending upon plant growth stage.

In order to map the captured TA images ($n = 32$) to root biomass, we process the reconstructed images as shown in Fig. 4a. The image processing steps involved include thresholding, edge detection, hole filling, smoothing and filtering to remove noise and artifacts to create a binary image of the potato tuber. We then extract the number of white pixels from the processed binary image and correlate that to the fresh weight of the potatoes as measured when they were first harvested. As Fig. 4b shows, a strong correlation exists between the

reconstructed, processed TA image and the fresh weight of the potatoes which serves as a proxy for biomass content.

V. CONCLUSION

In this work, we demonstrated the first experimental thermoacoustic images of plant material buried in soil, captured in a completely non-invasive and non-destructive manner. The images matched well with the ground-truth and extracted parameters showed strong correlation to root biomass. We also discussed the many degrees-of-freedom available due to the hybrid nature of the NCTA system as well as experimentally investigated the tradeoffs involved in using ultrasound sensors with different sensitivities and bandwidths.

Future work will seek to further improve the proposed system by deploying CMUT arrays instead of single elements and improving image resolution by using multi-frequency CMUTs [20]. Dynamic measurements of live plants, with finer root structures [23] will also be conducted in a variety of soil types. Additional below-ground parameters of interest will be extracted and mapped to captured thermoacoustic signals and images. Finally, the system will be deployed for below-ground imaging of root system architectures in the field.

ACKNOWLEDGMENT

The authors would like to thank Prof. B. T. Khuri-Yakub and his research group for providing the utilized CMUTs.

REFERENCES

- [1] S. McCouch, G. J. Baute, J. Bradeen, P. Bramel, P. K. Bretting, E. Buckler *et al.*, "Feeding the future," *Nature*, vol. 499, no. 7456, pp. 23–24, 2013.
- [2] A. Walter, F. Liebisch, and A. Hund, "Plant phenotyping: from bean weighing to image analysis," *Plant methods*, vol. 11, no. 1, pp. 1–11, 2015.
- [3] J. L. Araus and J. E. Cairns, "Field high-throughput phenotyping: the new crop breeding frontier," *Trends in plant science*, vol. 19, no. 1, pp. 52–61, 2014.
- [4] A. Chawade, J. van Ham, H. Blomquist, O. Bagge, E. Alexandersson, and R. Ortiz, "High-throughput field-phenotyping tools for plant breeding and precision agriculture," *Agronomy*, vol. 9, no. 5, p. 258, 2019.
- [5] L. Li, Q. Zhang, and D. Huang, "A review of imaging techniques for plant phenotyping," *Sensors*, vol. 14, no. 11, pp. 20 078–20 111, 2014.
- [6] J. A. Atkinson, M. P. Pound, M. J. Bennett, and D. M. Wells, "Uncovering the hidden half of plants using new advances in root phenotyping," *Current opinion in biotechnology*, vol. 55, pp. 1–8, 2019.
- [7] J. P. Lynch, "Roots of the second green revolution," *Australian Journal of Botany*, vol. 55, no. 5, pp. 493–512, 2007.
- [8] C. Costa, U. Schurr, F. Loreto, P. Menesatti, and S. Carpentier, "Plant phenotyping research trends, a science mapping approach," *Frontiers in plant science*, vol. 9, p. 1933, 2019.
- [9] A. Singhvi, K. C. Boyle, M. Fallahpour, B. T. Khuri-Yakub, and A. Arbabian, "A microwave-induced thermoacoustic imaging system with non-contact ultrasound detection," *IEEE transactions on ultrasonics, ferroelectrics, and frequency control*, vol. 66, no. 10, pp. 1587–1599, 2019.
- [10] B. Ma, K. Firouzi, K. Brenner, and B. T. Khuri-Yakub, "Wide bandwidth and low driving voltage vented CMUTs for airborne applications," *IEEE transactions on ultrasonics, ferroelectrics, and frequency control*, vol. 66, no. 11, pp. 1777–1785, 2019.
- [11] A. Singhvi, B. Ma, J. D. Scharwies, J. R. Dinneny, B. T. Khuri-Yakub, and A. Arbabian, "Non-contact thermoacoustic sensing and characterization of plant root traits," in *2019 IEEE International Ultrasonics Symposium (IUS)*. IEEE, 2019, pp. 1992–1995.
- [12] A. Delgado, D. B. Hays, R. K. Bruton, H. Ceballos, A. Novo, E. Boi, and M. G. Selvaraj, "Ground penetrating radar: a case study for estimating root bulking rate in cassava (*manihot esculenta crantz*)," *Plant methods*, vol. 13, no. 1, pp. 1–11, 2017.
- [13] L. V. Wang, *Photoacoustic imaging and spectroscopy*. CRC press, 2017.
- [14] W. E. Patitz, B. C. Brock, and E. G. Powell, "Measurement of dielectric and magnetic properties of soil," Sandia National Labs., Tech. Rep., 1995.
- [15] S. Nelson, "Frequency- and temperature-dependent permittivities of fresh fruits and vegetables from 0.01 to 1.8 GHz," *Transactions of the ASAE*, vol. 46, no. 2, p. 567, 2003.
- [16] J. A. Doolittle, F. E. Minzenmayer, S. W. Waltman, E. C. Benham, J. Tuttle, and S. Peaslee, "Ground-penetrating radar soil suitability map of the conterminous United States," *Geoderma*, vol. 141, no. 3-4, pp. 416–421, 2007.
- [17] A. Katz and M. Franco, "GaN comes of age," *IEEE microwave magazine*, vol. 11, no. 7, pp. S24–S34, 2010.
- [18] F. Benedetto and F. Tosti, "GPR spectral analysis for clay content evaluation by the frequency shift method," *Journal of Applied Geophysics*, vol. 97, pp. 89–96, 2013.
- [19] Y. Yongshuai, Y. Yajing, and Z. Guizhang, "Estimation of sand water content using GPR combined time-frequency analysis in the Ordos Basin, China," *Open Physics*, vol. 17, no. 1, pp. 999–1007, 2019.
- [20] A. Singhvi, A. Fitzpatrick, and A. Arbabian, "An Electronically Tunable Multi-Frequency Air-Coupled CMUT Receiver Array with sub-100 μ Pa Minimum Detectable Pressure Achieving a 28kb/s Wireless Uplink Across a Water-Air Interface," in *2022 IEEE International Solid-State Circuits Conference (ISSCC)*. IEEE, 2022.
- [21] N. Sanchez, K. Chen, C. Chen, D. McMahill, S. Hwang, J. Lutsky *et al.*, "An 8960-Element Ultrasound-on-Chip for Point-of-Care Ultrasound," in *2021 IEEE International Solid-State Circuits Conference (ISSCC)*. IEEE, 2021, pp. 480–482.
- [22] Z. Lu and J. M. Sabatier, "Effects of soil water potential and moisture content on sound speed," *Soil Science Society of America Journal*, vol. 73, no. 5, pp. 1614–1625, 2009.
- [23] A. Singhvi, M. L. Wang, A. Fitzpatrick, and A. Arbabian, "Multi-task learning for simultaneous speed-of-sound mapping and image reconstruction using non-contact thermoacoustics," in *2021 IEEE International Ultrasonics Symposium (IUS)*. IEEE, 2021, pp. 1–5.
- [24] B. Ma, K. Firouzi, K. Brenner, and B. T. Khuri-Yakub, "High sensitivity and wide bandwidth airborne cmuts with low driving voltage," in *2019 IEEE International Ultrasonics Symposium (IUS)*. IEEE, 2019, pp. 1201–1204.
- [25] N. Apte, K. K. Park, A. Nikoozadeh, and B. T. Khuri-Yakub, "Bandwidth and sensitivity optimization in cmuts for airborne applications," in *2014 IEEE International Ultrasonics Symposium*. IEEE, 2014, pp. 166–169.
- [26] M. Sautto, A. S. Savoia, F. Quaglia, G. Caliano, and A. Mazzanti, "A comparative analysis of CMUT receiving architectures for the design optimization of integrated transceiver front ends," *IEEE transactions on ultrasonics, ferroelectrics, and frequency control*, vol. 64, no. 5, pp. 826–838, 2017.
- [27] C. Chen and M. Pertijs, "Integrated transceivers for emerging medical ultrasound imaging devices: A review," *IEEE Open Journal of the Solid-State Circuits Society*, 2021.
- [28] G. Thomas and G. Sansonetti, *New light on a hidden treasure: international year of the potato 2008, an end-of-year review*. Food & Agriculture Org, 2009.
- [29] J. Wishart, T. S. George, L. K. Brown, P. J. White, G. Ramsay, H. Jones, and P. J. Gregory, "Field phenotyping of potato to assess root and shoot characteristics associated with drought tolerance," *Plant and soil*, vol. 378, no. 1, pp. 351–363, 2014.
- [30] R. Sugiura, S. Tsuda, S. Tamiya, A. Itoh, K. Nishiwaki, N. Murakami *et al.*, "Field phenotyping system for the assessment of potato late blight resistance using rgb imagery from an unmanned aerial vehicle," *Biosystems engineering*, vol. 148, pp. 1–10, 2016.
- [31] A. Haverkort and A. Verhagen, "Climate change and its repercussions for the potato supply chain," *Potato research*, vol. 51, no. 3, pp. 223–237, 2008.
- [32] M. Fallahpour, J. T. Case, M. T. Ghasr, and R. Zoughi, "Piecewise and wiener filter-based sar techniques for monostatic microwave imaging of layered structures," *IEEE Transactions on Antennas and Propagation*, vol. 62, no. 1, pp. 282–294, 2013.
- [33] D. Li, C. Quan, Z. Song, X. Li, G. Yu, C. Li, and A. Muhammad, "High-throughput plant phenotyping platform (ht3p) as a novel tool for estimating agronomic traits from the lab to the field," *Frontiers in Bioengineering and Biotechnology*, vol. 8, p. 1533, 2021.
- [34] J. Steinke, J. van Etten, A. Müller, B. Ortiz-Crespo, J. van de Gevel, S. Silvestri, and J. Priebe, "Tapping the full potential of the digital revolution for agricultural extension: an emerging innovation agenda," *International Journal of Agricultural Sustainability*, vol. 19, no. 5-6, pp. 549–565, 2021.